Reduction of persistent photoconductivity in ZnO thin film transistor-based UV photodetector

Pavel Ivanoff Reyes,[1] Chieh-Jen Ku,[1] Ziqing Duan,[1] Yi Xu,[2] Eric Garfunkel,[2] and Yicheng Lu[1,a)]
[1]*Department of Electrical and Computer Engineering, Rutgers University, Piscataway, New Jersey 08854-8058, USA*
[2]*Department of Chemistry and Chemical Biology, Rutgers University, Piscataway, New Jersey 08854-8058, USA*

(Received 1 April 2012; accepted 3 July 2012; published online 19 July 2012)

We report a ZnO-based thin film transistor UV photodetector with a back gate configuration. The thin-film transistor (TFT) aspect ratio W/L is 150 μm/5 μm and has a current on-off ratio of 10^{10}. The detector shows UV-visible rejection ratio of 10^4 and cut-off wavelength of 376 nm. The device has low dark current of 5×10^{-14} A. The persistent photoconductivity is suppressed through oxygen plasma treatment of the channel surface which significantly reduces the density of oxygen vacancy confirmed by XPS measurements. The proper gate bias-control further reduces recovery time. The UV-TFT configuration is particularly suitable for making large-area imaging arrays. © *2012 American Institute of Physics*. [http://dx.doi.org/10.1063/1.4737648]

ZnO is promising for UV detection due to its wide bandgap (~3.3 eV at room temperature), large exciton binding energy (~60 meV), and superior radiation hardness. Its bandgap can be extended through Mg incorporation in the ternary alloy $Mg_xZn_{1-x}O$ for deep UV sensitivity. So far, the research on ZnO-based UV photodetectors has been focused on the two terminal devices including photoconductive type[1–5] and Schottky type.[6–8] In addition, ZnO thin film transistor (TFT)-based UV photodetectors were also reported.[9–12] The TFT-based UV photodetector is a three-teminal device, which possesses intrinsic advantage of enabling biasing control over the two-terminal counterpart. Furthermore, the TFTs can be made on a large area of glass substrates, particularly suitable to make the photodetector-arrays for UV imaging applications. However, the previously reported ZnO-based TFT UV photodetectors suffered from poor performances, including the low mobility, high operating voltages, and especially, slow recovery speeds (24 ms recovery time for best results[12]) due to the persistent photoconductivity effects (PPC).[13,14]

In this letter, we report a ZnO TFT-based UV photodetector with a high UV-visible optical rejection ratio and low dark current and fast recovery time. The recovery time of the photodetector is improved by reduction of PPC through oxygen plasma treatment of the channel surface. Further PPC reduction is achieved through gate bias control.

The inset of Fig. 1(a) shows a schematic of a ZnO-TFT UV photodetector with the bottom gate configuration. The device was built on a heavily doped n-type Si substrate with a thermally grown SiO_2 layer (100 nm). The gate metallization scheme is Ti (100 nm)/Au (50 nm). The gate dielectric layer was made of PECVD-grown SiO_2 (~70 nm). The ZnO channel (~50 nm) was grown using metal-organic chemical vapor deposition (MOCVD) at 350 °C with DEZn (diethyl zinc) as the Zn precursor. The ZnO channel layer serves as the optically active layer. The source and drain electrodes are composed of Ti (100 nm)/Au (50 nm). The device has a

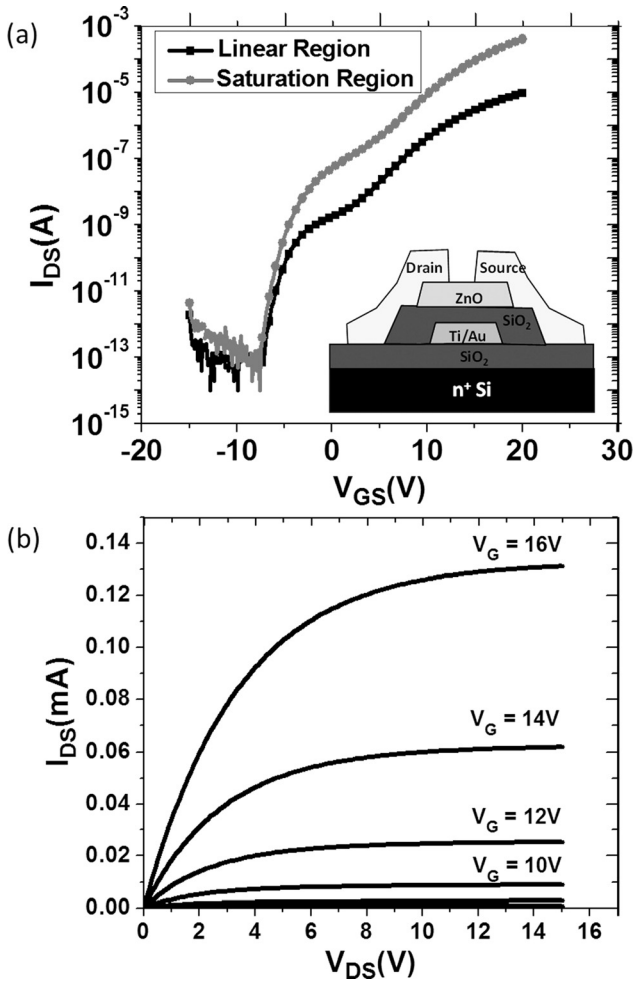

FIG. 1. Electrical characteristics in dark condition of the ZnO-TFT UV photodetector: (a) transconductance I_{DS}-V_{GS} curves, the inset shows the schematic of the device, and (b) transistor characteristic I_{DS}-V_{DS} curves.

a)Author to whom correspondence should be addressed. Electronic mail: ylu@rci.rutgers.edu.

nominal aspect ratio W/L = 150 μm/5 μm. The I-V characterizations were conducted in the dark using an HP-4156C semiconductor parameter analyzer at room temperature. The device operates in the enhancement mode with a threshold voltage of 1.17 V, a high field effect mobility μ_{FE} of 32.4 $cm^2/V\,s$, and an on-off ratio of 10^{10} as shown in both of the transconductance curves in Fig. 1(a) and the transistor characteristic curves in Fig. 1(b). As shown in Fig. 1(a), the dark current of the device (at −10 V gate bias) is 5×10^{-14} A. The spectral response of the ZnO-TFT UV photodetector was carried out through irradiating the exposed TFT channel using a broadband UV lamp with a tunable monochromator (Oriel Optics MS257). The wavelength was automatically varied from 290 nm to 600 nm with an input optical intensity at the device aperture equal to 1.6 mW/cm^2 while the I-V characteristics of the device was measured. The drain was biased with a constant voltage (V_{DD}) of +10 V. The transconductance I_{DS}-V_{GS} curve was measured for each wavelength and the drain current was monitored at gate voltage (V_{GS}) of −10 V. The resulting optical spectral response of the ZnO TFT UV photodetector is shown in Fig. 2(a). The 3-dB optical absorption bandwidth of the device is ~60 nm, while the rejection wavelength (at 20 dB point) is 376 nm, which corresponds to the bandgap of ZnO. Fig. 2(b) shows the transconductance curve of the device at 500 nm visible illumination and at 335 nm UV illumination (the peak wavelength). Under gate bias of −10 V, Fig. 2(b) shows ~10^4 UV-visible optical rejection ratio.

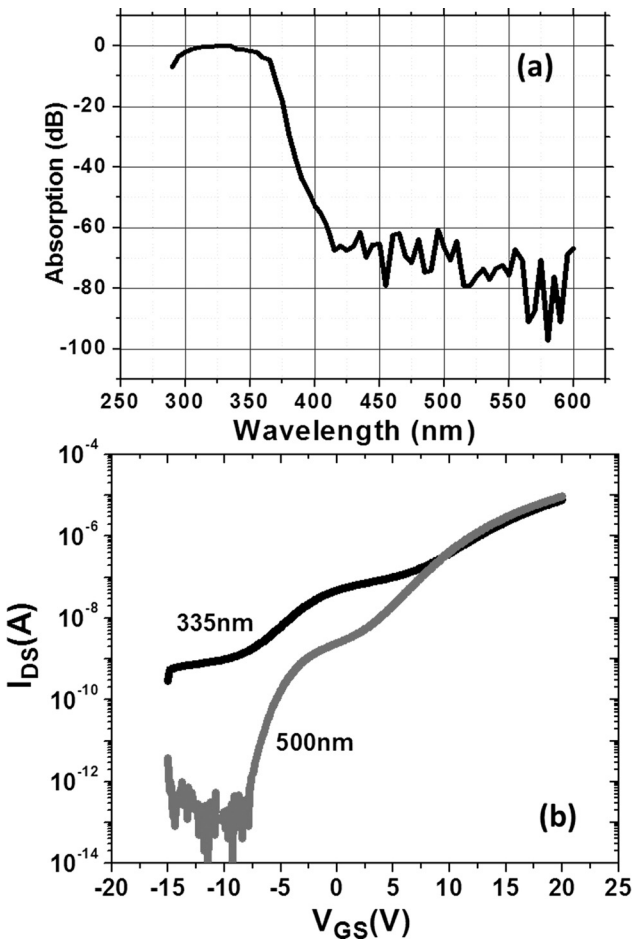

FIG. 2. (a) Spectral response of the ZnO-TFT UV photodetector, (b) photocurrents at visible (500 nm) and UV (335 nm) illumination showing optical rejection ratio of 10^4 at −10 V gate bias.

The temporal photoresponse of the ZnO TFT UV photodetector was measured using a Laser Science VSL 337ND-S nitrogen pulsed-laser as the optical source. It was operated at 40 ns optical pulse duration. The optical intensity at the device aperture is 2.4 $\mu W/cm^2$ averaged at 60 Hz. The laser wavelength is 337 nm which was externally triggered at 10% duty cycle burst mode. The measured turn-on time of the device is 400 μs, and a recovery time of 26 ms. This recovery time, though is comparable to the best previously reported ZnO TFT UV photodetectors (500 μs turn on time and 24 ms recovery time)[12] can be significantly improved through reduction of PPC via surface treatment and gate bias control.

The penetration depth of UV is ~50 nm at wavelengths near the peak absorption of ZnO (375 nm–340 nm).[15,16] This implies that the photo-generation happens not only on the surface of the ZnO channel but also within the bulk of the ZnO film. The slow photoresponse of ZnO during the recovery time is mainly due to the oxygen adsorption-photodesorption and defect related recombination processes.[17] This involves a two-step process: (i) under the dark conditions, oxygen adsorption happens at the surface states (oxygen vacancy sites) to create a negatively charged ion by capturing a free electron from *n*-type ZnO: $O_2 + e^- \rightarrow O_2^-$; (ii) under UV illumination, photodesorption of O_2 takes place where the negative oxygen ions capture the photogenerated holes that migrate toward the surface of ZnO: $h^+ + O_2^- \rightarrow O_2$. Therefore, the larger the concentration of oxygen vacancies at the surface of the ZnO channel, the slower the recovery time after UV illumination. To reduce the oxygen vacancies that are responsible for the slow recovery time of the photodetector, we performed a 3-min oxygen plasma treatment at 50 W on the channel surface of the ZnO-TFT. Figure 3(a) shows the turn-off times of the untreated device, and the device with oxygen plasma treatment. The surface treated device yielded a reduced turn-off time of 10 ms as compared to 26 ms turn-off time of the untreated device. The surface treated device also exhibited a higher generated photocurrent at 340 nm illumination. At −10 V gate bias (V_{GS}), the untreated device only generated ~10^{-6} A of photocurrent while the device with the plasma treatment showed ~10^{-4} A of photocurrent.

The improvement of the switching speed of the surface treated devices is attributed to the reduction of the oxygen vacancies near the surface of the ZnO channel. An x-ray photoelectron spectroscopy (XPS) spectrum analysis was performed on the devices to determine the extent of this reduction. Figures 3(b) and 3(c) show O_{1s} peaks in XPS spectra of the untreated ZnO channel and the O_2 plasma treated ZnO channel, respectively. Gaussian fitting was used in the deconvolution of the O_{1s} peaks. The XPS spectrum of the untreated ZnO channel shows two peaks: the peak appearing at the lower binding energy 530.68 eV (O_I) is due to O^{2-} ions present in the stoichiometric ZnO; on the other hand, the peak at the higher binding energy ~532.38 eV (O_{II}) can be attributed to O^{2-} ions in oxygen deficient ZnO.[18] The ratio of the peak area due to the oxygen deficient ZnO over the total area of the two peaks (O_{II}/O_{tot}) indicates the relative quantity of this oxygen-related defect. The untreated ZnO channel has a O_{II}/O_{tot} ratio of 29% while for

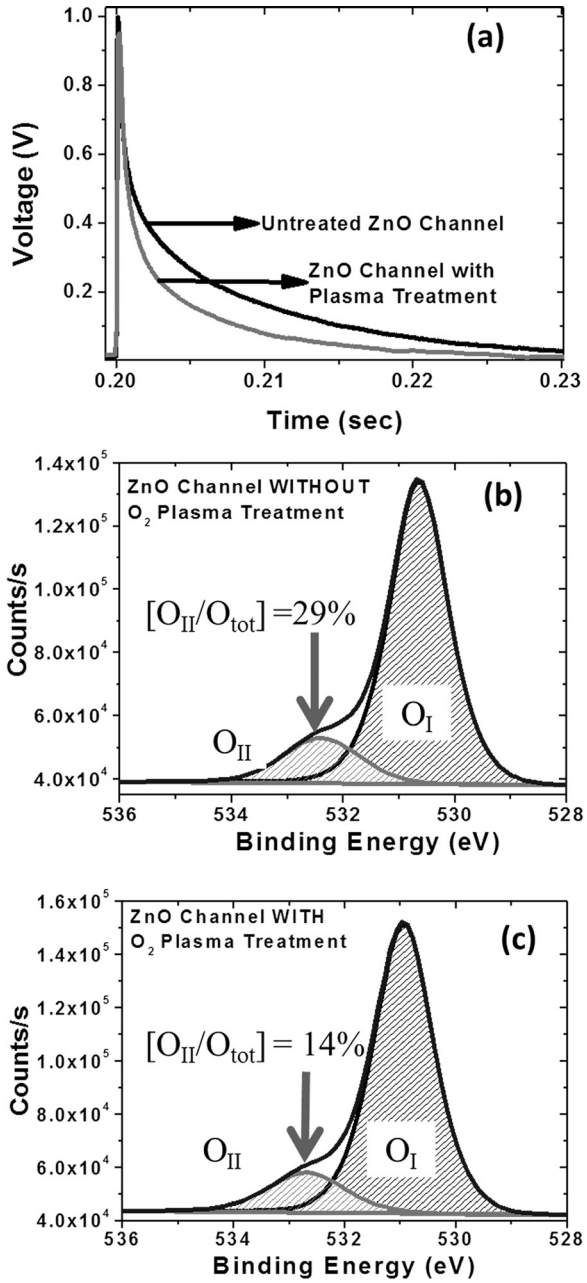

FIG. 3. (a) Recovery times of the ZnO-TFT UV photodetector with and without channel surface treatment; XPS spectra of (b) untreated ZnO channel, and (c) oxygen plasma-treated ZnO channel.

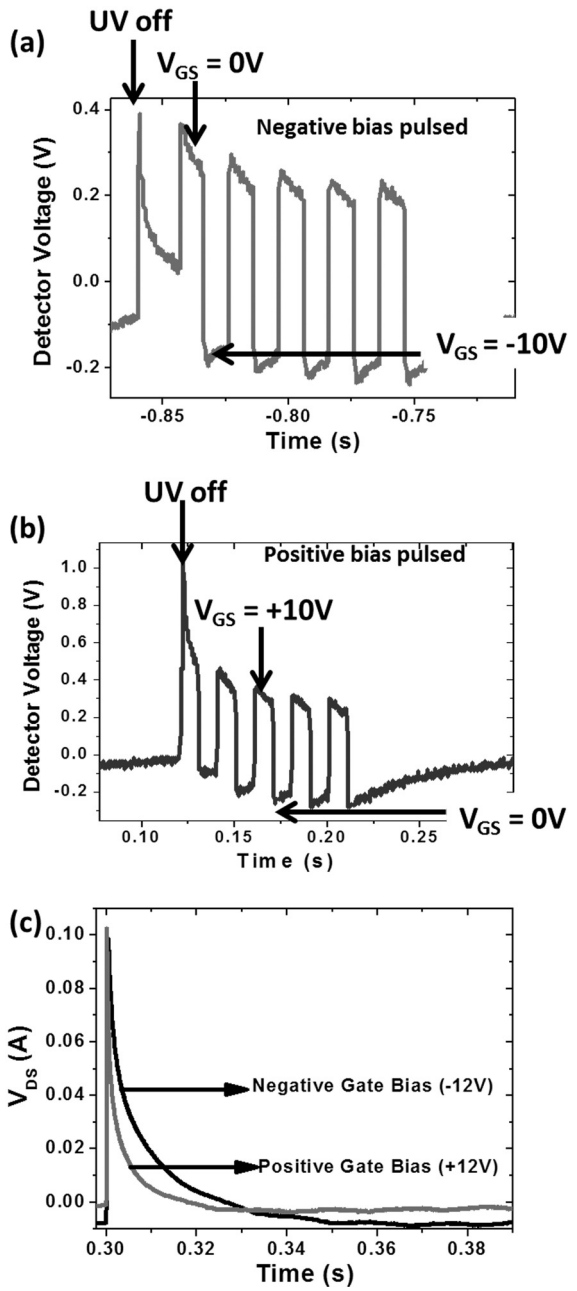

FIG. 4. (a) Slow recovery mechanism in the ZnO-TFT UV photodetector with negative pulsed gate biasing; (b) suppression of the PPC when the photodetector is pulsed with positive gate bias; (c) turn-off times of the ZnO-TFT UV photodetector for both the reverse and positive gate bias.

the channel with oxygen plasma treatment, the O_{II}/O_{tot} ratio has significantly reduced to 14%. The temporal stability of the oxygen plasma treatment on the ZnO channel depends on the storage and passivation of the device. No appreciable degradation was observed on the ZnO channel within ~7 days if the unpassivated devices were kept in a sealed package at room temperature. This is mainly because the oxygen in the air will start to react with the surface of the channel. However, the devices will keep the oxygen-plasma treatment conditions almost indefinitely as long as the devices are passivated with a coating of photoresist.

The further improvement of the recovery time was realized through positive biasing of the gate of the ZnO-TFT UV photodetector. To show the negative and positive gate bias effect on the decay of the photocurrent, we performed the pulsed-gate photoconductivity testing. The testing involves pulsing the gate voltage immediately after the UV illumination is turned off and then the drain voltage is monitored. For the negative gate bias test, we pulsed the gate with −10 V to 0 V at 10 Hz after the UV light was shut off. As shown in Fig. 4(a), the photocurrent does not decay quickly even after the UV light is turned off due to persistent photoconductivity. For the positive gate bias test, where the pulsed gate bias varied between 0 V and +10 V at 10 Hz after the UV light was shut off. As shown in Fig. 4(b), the photocurrent decays fast after the UV light is turned off due to suppression of persistent photoconductivity. Fig. 4(c) shows that the positive gate bias reduces the switch off time to 5 ms, in comparison to the negative-biased device with a turn off time of 29 ms. Gate bias control significantly decreases the recovery time.

The slowing down of the recombination process is precipitated by the separation of the UV-generated electron-hole pairs due to the large depletion region created by the negative gate bias. On the other hand, the positive bias at the TFT gate provides a conduction path for the separated charges to drain out of the channel. The control of recovery time through the proper gate biasing provides the most suitable way for the ZnO TFT UV photodetector to be used as an active element into a UV imaging array. Such a configuration possesses the intrinsic advantage as a three-terminal photodetector, where UV illumination will serve as the "write" function, the positive gate bias as the "clear" function, and the negative gate bias as the "store" function.

In conclusion, we reported a ZnO UV photodetector based on a thin film transistor with a back gate configuration. The UV photodetector has an electrical on-off ratio of 10^{10}, UV-visible optical rejection ratio of 10^4, rejection wavelength of 376 nm, and a low dark current of 5×10^{-14} A. The improvement of recovery time for the photodetector was achieved through two routes: the suppression of persistent photoconductivity using oxygen plasma treatment of the ZnO channel to reduce the oxygen vacancies which is confirmed, and positive gate biasing control. The combination of these two methods improved the recovery time to 5 ms.

This work has been supported in part by the AFOSR under FA9550-08-01-0452 and by the NSF under ECCS 1002178 and DMR-1006740.

[1]Q. A. Xu, J. W. Zhang, K. R. Ju, X. D. Yang, and X. Hou, J. Cryst. Growth **289**, 44–47 (2006).
[2]H. Kind, H. Yan, B. Messer, M. Law, and P. Yang, Adv. Mater. **14**(2), 158–160 (2002).
[3]K. W. Liu, J. G. Ma, J. Y. Zhang, Y. M. Lu, D. Y. Jiang, B. H. Li, D. X. Zhao, Z. Z. Zhang, B. Yao, and D. Z. Shen, Solid-State Electron **51**, 757–761 (2007).
[4]C. Soci, A. Zhang, B. Xiang, S. A. Dayeh, D. P. R. Aplin, J. Park, X. Y. Bao, Y. H. Lo, and D. Wang, Nano Lett. **7**(4) 1003–1009 (2007).
[5]Y. Liu, C. R. Gorla, S. Liang, N. Emanetoglu, Y. Lu, H. Shen, and M. Wraback, J. Electron. Mater. **29**, 69 (2000).
[6]S. Liang, H. Sheng, Y. Liu, Z. Huo, Y. Lu, and H. Shen, J. Cryst. Growth **225**, 110 (2001).
[7]L. Luo, Y. Zhang, S. S. Mao, and L. Lin, Sens. Actuators A **127**, 201–206 (2006).
[8]D. Jiang, J. Zhang, Y. Lu, K. Liu, D. Zhao, Z. Zhang, D. Shen, and X. Fan, Solid-State Electron **52**, 679–682 (2008).
[9]K. Lee, K.-T. Kim, J.-M. Choi, M. S. Oh, D. K. Hwang, S. Jang, E. Kim, and S. Im, J. Phys. D: Appl. Phys. **41**, 135102 (2008).
[10]H. S. Bae, M. H. Yoon, J. H. Kim, and S. Im, Appl. Phys. Lett. **83**(25), 5313–5315 (2003).
[11]H. S. Bae, C. M. Choi, J. H. Kim, and S. Im, J. Appl. Phys. **97**, 076104 (2005).
[12]H. Bae, S. Im, and J. Song, Jpn. J. Appl. Phys. **47**(7), 5362–5364 (2008).
[13]S. Lany and A. Zunger, Phys. Rev. B **72**, 035215 (2005).
[14]K. Ghaffarzadeh, A. Nathan, J. Robertson, S. Kim, S. Jeon, C. Kim, U.-I. Chung, and J.-H. Lee, Appl. Phys. Lett. **97**, 143510 (2010).
[15]T. M. Børseth, B. G. Svensson, A. Y. Kuznetsov, P. Klason, Q. X. Zhao, and M. Willander, Appl. Phys. Lett. **89**, 262112 (2006).
[16]J. F. Muth, R. M. Kolbas, A. K. Sharma, S. Oktyabrsky, and J. Narayan, J. Appl. Phys. **85**(11), 7884–7887 (1999).
[17]Y. Takahashi, M. Kanamori, A. Kondoh, H. Minoura, and Y. Ohya, Jpn. J. Appl. Phys. **33**, 6611 (1994).
[18]Y. S. Rim, D. L. Kim, W. H. Jeong, and H. J. Kim, Appl. Phys. Lett. **97**, 233502 (2010).